Open-Loop End-to-End Transmission for Multihop Opportunistic Networks With Energy-Harvesting Devices

I-Wei Lai, *Member, IEEE*, Chia-Han Lee, *Member, IEEE*, Kwang-Cheng Chen, *Fellow, IEEE*, and Ezio Biglieri, *Life Fellow, IEEE*

***Abstract*— Networks formed by energy-harvesting devices impose new technological challenges on data transmission due to uncertainty of the amount of energy that can be harvested. This is even more challenging with multihop networks, in which transmission outage occurs when one single device along the relay path cannot harvest enough energy. A virtual multiple-input multiple-output (MIMO) model for multihop, multipath networks has recently been developed to facilitate reliable open-loop end-to-end transmissions, making networks robust to random transmission outages without the necessity of bandwidth-consuming and complicated end-to-end feedback and control. In this paper, a framework based on a virtual MIMO model of multihop, multipath opportunistic networks formed by energy-harvesting devices is developed. We propose rotated-algebraic path-time codes (RA-PTC), by which data are encoded using Givens rotation and cyclic division algebras. Without rate loss, a form of time diversity is exploited by repeatedly transmitting the RA-PTC-coded data. Extensive theoretical analyses are carried out using amount of fading and diversity as metrics. Both the performance enhancement due to the proposed RA-PTC and the performance loss due to energy shortage are quantified. Furthermore, a simple yet effective cyclic power control is proposed to improve transmission reliability. Numerical results demonstrate that RA-PTC and cyclic power control enable efficient and reliable end-to-end transmission in multipath, multihop opportunistic networks formed by energy-harvesting devices.**

***Index Terms*— Multiple-input multiple-output (MIMO), virtual MIMO, path-time code (PTC), open-loop communication, slow-fading, erasure, energy harvesting, cyclic division algebra, power control.**

Manuscript received November 15, 2015; revised March 21, 2016; accepted May 20, 2016. Date of publication June 1, 2016; date of current version July 12, 2016. I-Wei Lai was supported by Ministry of Science and Technology (MOST) under the grant 104-2218-E-182-004. Chia-Han Lee is supported by MOST, Taiwan under grant MOST104-2221-E-001-013-MY2. Kwang-Cheng Chen is supported under grant NSC102-2221-E-002-016-MY2. The work of Ezio Biglieri was supported by Project TEC2015-6628-P. The associate editor coordinating the review of this paper and approving it for publication was W. Zhang.

I.-W. Lai is with the Department of Electronic Engineering, Chang Gung University, Taoyuan 333, Taiwan (e-mail: iweilai0924@gmail.com).

C.-H. Lee is with the Research Center for Information Technology Innovation, Academia Sinica, Taipei 11529, Taiwan (e-mail: chiahan@citi.sinica.edu.twb).

K.-C. Chen is with the Graduate Institute of Communication Engineering, National Taiwan University, Taipei 10617, Taiwan (e-mail: ckc@ntu.edu.tw).

E. Biglieri is with the Department of Information and Communications Technologies (DTIC), Universitat Pompeu Fabra, 08018 Barcelona, Spain, and also with the Electrical Engineering Department, University of California at Los Angeles, Los Angeles, CA 90095 USA (e-mail: e.biglieri@ieee.org).

Color versions of one or more of the figures in this paper are available online at http://ieeexplore.ieee.org.

Digital Object Identifier 10.1109/TCOMM.2016.2574858

I. Introduction

INSTEAD of being powered by a stable energy source, a device of energy-harvesting capability is able to collect energy from ambient environments through piezoelectricity, light, vibration, thermal difference, etc. For networks suffering from power supply problems, the network lifetime can be significantly prolonged through energy harvesting. However, the communication constraints imposed by energy harvesting, caused by the uncertainty of energy arrival, call for new system designs. In the past few years, point-to-point and relay communication of energy-harvesting devices have been well-studied [1]–[12], but how to achieve reliable end-to-end transmission in multihop networks with energy-harvesting devices remains an open problem.

Closed-loop communication systems utilize feedback for transmission control (e.g., power control, scheduling, and retransmission) and are widely adopted in existing communication standards. However, closed-loop communication requires a reliable end-to-end control channel for control message exchange between source and destination nodes. When a network scales, e.g., when the number of hops in a network increases, the construction of the end-to-end control channel becomes impractical, in particular for networks formed by energy-harvesting devices. On the contrary, *open-loop* communication systems, which take advantage of forward error control mechanisms and renounce to end-to-end feedback, have the potential of delivering good performance and efficiency under stringent link conditions [13]–[15], such as link disruption caused by energy shortage (i.e., the case when a device cannot harvest enough energy to relay data).

One promising approach to achieving open-loop communication is by applying the virtual multiple-input multiple-output (MIMO) technology to the network/session layer [16]–[20]. By encoding data along both path and time coordinates in a multipath, multihop network setting [21]–[23] using either a path-time code (PTC) [16], [17] or a path-permutation code (PPC) [18], error-resilient transmission without end-to-end feedback control can be achieved. This virtual MIMO-based open-loop physical communication technology has been successfully applied to ad hoc cognitive radio networks [17]. However, how to apply this virtual MIMO-based open-loop communication to networks with energy-harvesting devices has never been discussed in the literature.

Considering the different characteristics of cognitive radio networks and the networks formed by energy harvesting devices, a new framework and novel schemes are called for.

In this paper, a framework based on the application of virtual MIMO to multihop, multipath networks formed by energy-harvesting devices is proposed. Unlike [17], the slow-fading channel model is used for the environment of static energy-harvesting devices.[1] The event of a relay node being unable to harvest sufficient energy for transmission is modeled as an erasure, and the erasure statistics are derived according to the channel capacity and the energy arrival statistics. With this framework, a rotated-algebraic path-time code (RA-PTC) based on Givens rotation and cyclic division algebra [24], [25] is proposed to enable the exploitation of time diversity without causing rate loss. The diversity gain of RA-PTC is analyzed by deriving the pairwise error probability (PEP), and it is analytically shown that RA-PTC not only provides a superior diversity gain but also mitigates the performance degradation caused by multihop transmissions [26]. The severity of fading is then quantified by using the *amount of fading* performance parameter [26], [27]. Our analysis shows that when RA-PTC is used, the amount of fading for multihop transmission is reduced and approaches that for single-hop transmission. Furthermore, a cyclic power control is designed to enhance transmission reliability. The proposed power control has low complexity and can be distributedly implemented without any information exchange among nodes. A closed-form expression of the expected diversity gain obtained by using the proposed RA-PTC with cyclic power control is then provided. To the best of authors' knowledge, this is the first work that theoretically analyzes the diversity gain in the context of fading channel with random erasures. Finally, numerical examples demonstrate the effectiveness of our approach to multihop, multipath networks formed by energy-harvesting devices.

Space–time codes have been applied in the relay network, where the receiver is an energy-harvesting device [7], [28], [29]. Novel techniques are proposed to enhance the performance by exploiting the channel information at both transmission sides. Contrarily, the fundamental difference of this work lies in the fact that we remove all the end-to-end control and information exchange, leading to an open-loop communication. The erasure model is used to characterized the impairment caused by insufficient harvested energy. Such simple model is scalable and allows us to investigate a more complicated scenario where not only the destination node but also the source and relay nodes are energy-harvesting devices. Then, the RA-PTC is designed as tailored to such channel, together with the associated performance analysis.

In a nutshell, the proposed virtual MIMO RA-PTC architecture and cyclic power control combat the transmission outages caused by energy shortage without needing end-to-end feedback control and information exchange, thus resulting in a reliable and efficient open-loop end-to-end transmission. The contributions of this work are listed below:

① Proposal and realization of open-loop communication in multihop, multipath opportunistic networks formed by energy-harvesting devices.

② Design of RA-PTC based on the algebraic code and Givens rotation to mitigate erasures caused by insufficient harvested energy.

③ Design of the distributed cyclic power control to efficiently enhance transmission reliability without the necessity of global information exchange.

④ Theoretical analyses of end-to-end RA-PTC transmission with cyclic power control, including the closed-form expression of the diversity in fading channels with erasures.

This paper is organized as follows. Section II describes the system model and the virtual MIMO framework for multihop, multipath networks formed by energy-harvesting devices. In Section III, RA-PTC is illustrated, and in Section IV a low-complexity distributed cyclic power control is described. Then in Section V, diversity and the amount of fading of the proposed scheme are analyzed. Section VI provides numerical results to validate the analyses and to demonstrate the performance of the proposed virtual MIMO RA-PTC for networks formed by energy-harvesting devices over slow-fading channels. Finally, conclusions are drawn in Section VII.

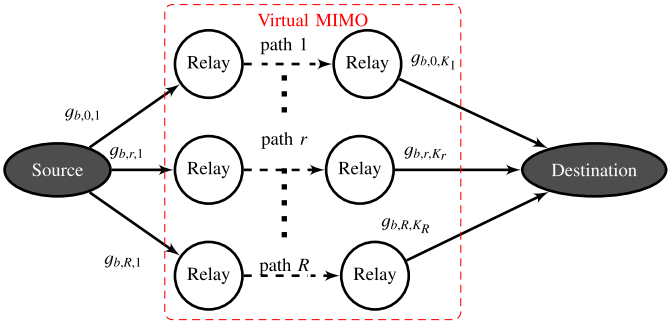

Fig. 1. Topology of the disjoint multipath end-to-end transmission in multihop networks formed by energy-harvesting devices.

II. System Model

In this work, the *disjoint multipath relay network* [16]–[20] is considered. Specifically, defining a *link* as a connection between two nodes and a *path* as an end-to-end connection between source and destination, the multipath relay is formed by R link-disjoint paths [30], [31], each including $K_r - 1$ relay nodes, $r \in \{1, \ldots, R\}$. This relay network can be established by using the routing algorithms in [21]–[23]. Fig. 1 illustrates the equivalent directed-graph model of such disjoint multipath relay network topology as an example. The link-disjoint model includes the possibility that a relay node is utilized by more than one path. When links in link-disjoint model fail, they often fail independently, except when a node moves out of range, which causes multiple links from/to the

[1] Although in some scenarios energy-harvesting devices may move around (for example, the case of wearables) and the channel is better modeled as fast-fading under that scenario, in this paper we target more common cases of static energy-harvesting devices. If it is required to consider the fast-fading channel, then the techniques developed in [17] can be applied on top of the framework developed in this paper.

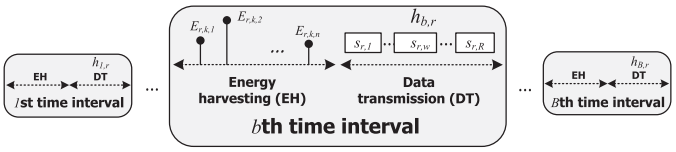

Fig. 2. Operation phases of the kth relay node in the rth relay path.

node fail together. The relays in different paths can transmit *simultaneously* since the availability of any two links in two different paths is independent by the definition of link-disjoint path. When the source node simultaneously transmits signals through multiple link-disjoint paths, inter-path interference may be introduced. Techniques are proposed on top of the disjoint paths, e.g., directional antennas, selection mechanism for inter-path interference minimization, and transmissions in different frequencies [32]–[34]. Consequently and for the sake of simplicity, in this work we neglect the inter-path interference. Note that when the severe inter-path interference occurs, the resulting transmission outage can be modeled by erasures, which are able to be mitigated by the technologies proposed in this work.

We assume that all nodes in the network rely on energy harvesting to acquire energy and all of them are equipped with a battery. When sufficient energy is collected at the source node, data is encoded along time and path coordinates using PTC, and the virtual MIMO transmission is initiated. The coded data is then transmitted to different relay paths,[2] and the coded data in each relay path is *amplified and forwarded* toward the destination node. The time interval is split into R discrete time instants and the coded data amplified and forwarded along the rth path is formed by encoding the data $\mathbf{x}$ by $\mathbf{s}_r(\mathbf{x}) = [s_{r,1}(\mathbf{x}), \ldots, s_{r,R}(\mathbf{x})]^\top$, where $(\cdot)^\top$ denotes the transpose operation. Since nodes need to harvest energy for data transmission, each relay node operates in two phases: the *energy-harvesting phase* and the *data transmission phase*, as illustrated in Fig. 2. During the energy-harvesting phase, a relay node charges its battery by collecting the energy from ambient environment. Here, we consider a rather complex case where the energy arrival follows the compound Poisson random process [1]. In particular, letting $E_{b,r,k,i}$ be the value of the ith energy arrival at the kth node in the rth relay path, and $E_{b,r,k}$ be the accumulated energy this node harvests in the bth time interval, we have

$$E_{b,r,k} = \sum_{i=1}^{n} E_{b,r,k,i}, \tag{1}$$

where the number of energy arrivals $n \in \mathbb{N}$ follows the Poisson distribution and $E_{b,r,k,i}$ is an independent identically-distributed (i.i.d.) random variable with respect to all indices [1]. We assume in this work that at the beginning of the energy harvesting phase, batteries are empty.[3] For the case where the batteries are initially non-empty, the performance analyzed and demonstrated in this work can serve as a lower bound since the accumulated harvested energy is larger in that case. During the data transmission phase, the relay node waits for the coded data, then amplifies and forwards the coded data to its next node until the depletion of its harvested energy. It should be emphasized that, since energy is crucial in networks relying on energy harvesting, the amplify-and-forward protocol is preferable to the decode-and-forward one since there is no power consumed on decoding when amplify-and-forward is applied. With the amplify-and-forward protocol, we can assume that the energy spent on the reception of coded data is negligible compared with the energy required for transmission.

When the harvested energy is insufficient, only part of the coded data can be transmitted and the rest is discarded. This results in transmission outage and this phenomenon can be modeled as an *erasure*. Let us define $\mathbf{V}_b \in \{0,1\}^{R\times R}$ as the erasure matrix used to characterize the transmission outage in the bth time interval. Specifically, if $s_{r,w}$ is lost in the bth time interval due to energy insufficiency, the entry $v_{b,r,w} \in \mathbf{V}_b$ is 0; otherwise, $v_{b,r,w}$ is 1. If we assume that in the bth time interval, the minimal harvested energy of the relay nodes in the rth relay path allows the transmission of the first w' symbols in the coded data $\mathbf{s}_r(\mathbf{x})$, then

$$v_{b,r,w} = \begin{cases} 1, & w \le w', \\ 0, & w > w', \end{cases} \tag{2}$$

which can be modeled as a Bernoulli-distributed random variable whose statistics depends on the energy harvesting results.

Now, let us define the link gain $g_{b,r,k}$ as the kth link in the rth path and the bth *time interval* with length equal to the duration of a coded data transmission. A slow-fading channel is considered, in which the fading gains $g_{b,r,k}$ remain constant in the duration of data transmission and the fading gains may change for different time intervals [1]. This channel model is practical since we consider static energy-harvesting devices and the energy harvesting phase is generally much longer than the data transmission phase. Cascaded by K_r links, the fading gain of the rth relay path in the bth time interval is given by

$$h_{b,r} = \prod_{k=1}^{K_r} g_{b,r,k}. \tag{3}$$

It is also assumed that the length of the time instant is longer than the end-to-end delay, so that the transmissions of $s_{r,w}$ and $s_{r,w+1}$ do not overlap. Then the received data in the bth time interval can be expressed as[4]

$$\mathbf{y}_b = [\mathbf{s}_1(\mathbf{x}), \ldots, \mathbf{s}_R(\mathbf{x})] \circ \mathbf{V}_b\mathbf{h}_b + \sum_{r=1}^{R} \tilde{\mathbf{n}}_{b,r} = \mathbf{S}(\mathbf{x}) \circ \mathbf{V}_b\mathbf{h}_b + \mathbf{n}_b, \tag{4}$$

where $\circ$ denotes the Schur product, $\mathbf{h}_b = [h_{b,1}, \ldots, h_{b,R}]^\top$, and $\mathbf{S}$ is the coded data. The additive white Gaussian

[2]This can be done by applying multiplexing techniques or the two-step protocol [35].

[3]In practical scenarios, batteries suffer from energy leakage due to imperfect storage [3], [4] and the circuits of the relay nodes consume energy even in the standby mode [5], [9]. Therefore, although the batteries may have residual energy from the previous transmission, we can reasonably assume that the batteries are empty at the beginning of the energy-harvesting phase.

[4]Although for ease of exposition we only consider the case where the length of the coded data equals the number of relay paths (as in [16]–[20]), more general cases can be easily dealt with.

noise (AWGN) $\tilde{\mathbf{n}}_{b,r}$ is the noise aggregated from all links in the rth path. Due to the amplifications of relay nodes and relay link gains, $\tilde{\mathbf{n}}_{b,r}$ has a different variance for each r and b [35]. Therefore, $\mathbf{n}_b$, the summation of $\tilde{\mathbf{n}}_{b,r}$ for $r = 1, \ldots, R$, also has time-varying noise power spectral density $N_{0,b}$ [17]. Please note that the time jitter due to imperfect synchronization of the system results in performance loss equivalent to loss of effective harvested energy or even discard of the transmitted symbols. Such potential transmission outages caused by both impairments can be characterized by erasures, which are mitigated by the proposed techniques in this work. In other words, compared with the conventional systems that design for channels without erasures, our study accommodates less strict synchronization algorithms by considering the effects of erasures and thus mitigation of its impacts. Moreover, although the signals propagated from various paths may have different delays, by setting the period of each time instant equal to the maximum delay, the destination node can accumulate all the incoming signals. In this case, the signals from all paths can be successfully collected and then inter-symbol interference is avoided.

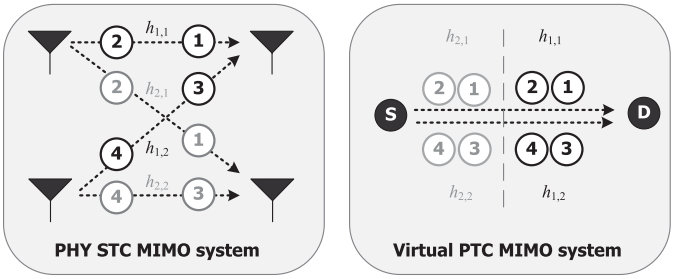

Fig. 3. Analogy between the physical-layer MIMO with an STC and the virtual MIMO with a PTC. The symbols labeled by '1' and '2' are transmitted from the first transmit antenna (first relay path) for the physical-layer MIMO system (virtual MIMO system); likewise, those labeled by '3' and '4' are transmitted from the second transmit antenna (second relay path) for the physical-layer MIMO system (virtual MIMO system). The symbols represented by black circles are received by the first receive antenna (in the first time interval) for the physical-layer MIMO system (virtual MIMO system); similarly, those represented by grey circles are received by the second receive antenna (in the second time interval). Thus, we can map transmit antennas to relay paths and receive antennas to time intervals. As the receiver and destination node first receive data transmitted in the 1st time interval experiencing $h_{1,1}$ and $h_{1,2}$, the figure is drawn in the way that the signals are chronologically from right to left, i.e., from the viewpoint of the receiver and destination node.

III. Rotated-Algebraic Path-Time Code

In [16]–[20], PTCs have been introduced to yield diversity gain and consequently to enhance the end-to-end transmission reliability in fast-fading channels. In this section, we propose a novel PTC for multihop, multipath networks formed by energy-harvesting devices over slow-fading channels. As shown in (4), end-to-end multipath transmission within a certain time interval can be modeled as a space-time coded (i.e., PTC-coded) multiple-input single-output (MISO) system with R time instants, R transmit antennas, and single receive antenna. It is well known that by applying the structure of space-time code (STC), a diversity gain of R can be achieved [36]. The diversity of an end-to-end PTC transmission in the context of R relay paths and B time intervals can be further increased up to RB, as will be introduced in next subsections and further analyzed in Sec. V.

A. Repetition Transmission

In RA-PTC, data $\mathbf{x}$ are encoded into $\mathbf{S}(\mathbf{x})$, and $\mathbf{S}(\mathbf{x})$ is repeatedly transmitted B times in B time intervals. Such repetition transmission can be interpreted as the result of having B *virtual* receive antennas. The relationship between the physical-layer STC MIMO system and the PTC-based virtual MIMO system is illustrated in Fig. 3, which uses a 2×2 MIMO as an example. In both cases, eight symbols are transmitted through four independently faded channels, and two coded symbols are concurrently received by the destination node (or receive antennas) at each time instant. Therefore, the received data in the bth time interval is given by

$$\mathbf{y}_b = \mathbf{S}(\mathbf{x}) \circ \mathbf{V}_b \mathbf{h}_b + \mathbf{n}_b, \qquad b = 1, \ldots B, \tag{5}$$

where the introduced time diversity results in a diversity gain up to RB, as in a physical-layer MIMO system with numbers of transmit and receive antennas both equal to R [36]. The temporal correlation between the successive time interval can be mapped to the PHY layer STC-MIMO system with *spatial correlation*, which has been widely investigated in literatures, e.g., [37], [38]. In the case of high temporal correlation, we can reduce the correlation by interleaving the repetitive transmissions of various data. Take two data $\mathbf{x}_1$ and $\mathbf{x}_2$ and $R = B = 2$ as an example. Instead of transmitting $\mathbf{S}(\mathbf{x}_1)$ repeatedly at the first and second time intervals, $\mathbf{S}(\mathbf{x}_1)$ and $\mathbf{S}(\mathbf{x}_2)$ are transmitted respectively and such transmission is repeated at the third and fourth time intervals. By applying this technique, the temporal correlation is reduced at the expense of larger transmission latency.

It should be emphasized that the throughput of this repetition transmission using multiple time intervals is not sacrificed. In particular, either the PTC designed for fast-fading channels or the conventional repetition transmission encodes $\mathbf{x}$ with length R [16], [17]. Assuming R time instants in one time interval, their throughputs are both one data symbol per time instant. For the repetition transmission using B time intervals, we encode a longer data $\mathbf{x}$ with length RB into the coded data with the same size as that in the fast-fading channel. Therefore, the throughput is one data symbol per time instant as well. In the next two subsections, we elaborate on the code design based on the cyclic division algebra [24], [25] and the Givens rotation, respectively.

B. Algebraic Code Construction

For the physical-layer MIMO system, cyclic division algebras are a powerful mathematical tool for the construction of a perfect STC which simultaneously achieves maximal throughput and diversity. We refer the readers to [25] for additional details of the cyclic division algebra. Here, we focus on code construction. For ease of exposition, the case of $R = B$ is considered as an example, so that the length of data $\mathbf{x}$ is R^2.

TABLE I
NUMERICAL FORMS OF THE ALGEBRAIC CODE GENERATING MATRIX

R	$\mathbf{M}$
2	$\begin{bmatrix} 0.477-0.276j & 0.724-0.447j \\ 0.477+0.724j & -0.276-0.447j \end{bmatrix}$
3	$\begin{bmatrix} 0.660+0.327j & 0.021+0.327j & -0.492+0.327j \\ -0.294-0.146j & -0.037-0.590j & -0.614+0.408j \\ 0.530+0.263j & -0.047-0.736j & -0.273-0.182j \end{bmatrix}$
4	$\begin{bmatrix} 0.26-0.31j & 0.35-0.42j & -0.42+0.51j & -0.21+0.26j \\ 0.26+0.08j & 0.47+0.16j & 0.16+0.05j & 0.76+0.26j \\ 0.26+0.24j & -0.51-0.42j & -0.42-0.35j & 0.31+0.26j \\ 0.26-0.76j & -0.05+0.16j & 0.16-0.47j & -0.09+0.26j \end{bmatrix}$

For the encoding process, the data $\mathbf{x}$ is first partitioned into R groups, each having R elements, i.e., the ith group comprises entries $[x_{Ri+1}, \ldots, x_{Ri+R}]$. Then, every group is individually encoded by using the code generating matrices $\mathbf{M}$ listed in Table I. The encoded sequence is then located diagonally in the algebraic coded data $\tilde{\mathbf{S}}(\mathbf{x})$. This encoding procedure can be mathematically formulated as

$$\tilde{\mathbf{S}}(\mathbf{x}) = \sum_{i=0}^{R-1} \mathrm{diag}\left(\mathbf{M} \begin{bmatrix} x_{Ri+1} \\ \vdots \\ x_{Ri+R} \end{bmatrix} \right) \mathbf{E}(R)^i, \tag{6}$$

where $\mathrm{diag}(\mathbf{a})$ is a diagonal matrix with diagonal entries being $\mathbf{a}$. $\mathbf{E}(R)^i$ is the ith power of the matrix $\mathbf{E}(r)$, i.e., the repeated multiplications with i times. The matrix $\mathbf{E}(R)$ is used to allocate the encoded sequences to $\tilde{\mathbf{S}}(\mathbf{x})$. Specifically, the (p, q)th entry of $\mathbf{E}(R)$ is defined as

$$E_{p,q}(R) = \begin{cases} 1, & \text{if } p = q+1, \\ j, & \text{if } p = R,\ q = 1, \\ 0, & \text{otherwise.} \end{cases}$$

By multiplying $\mathbf{E}(R)^i$, the encoded sequence associated with $[x_{Ri+1}, \ldots, x_{Ri+R}]^\top$ is located on the cyclic-shifted diagonal lines, i.e., $\tilde{S}(\mathbf{x})_{p,\ \mathrm{mod}\ (p+i,R)}$ entries for $p = 1, \ldots, R$, where $\mathrm{mod}\ (\cdot, R)$ denotes modulo-R reduction.

Considering a toy example with $(R, B) = (2, 2)$, data $\mathbf{x} = [x_1, \ldots, x_4]$, $\theta = \frac{1+\sqrt{5}}{2}$, $\bar{\theta} = 1 - \theta = \frac{1-\sqrt{5}}{2}$, $\alpha = 1 + j(1-\theta)$, and $\bar{\alpha} = 1 + j(1-\bar{\theta})$, the algebraic code $\tilde{\mathbf{S}}(\mathbf{x})$ is computed by

$$\tilde{\mathbf{S}}(\mathbf{x}) = \mathrm{diag}\left(\mathbf{M} \begin{bmatrix} x_1 \\ x_2 \end{bmatrix} \right) \begin{bmatrix} 1 & 0 \\ 0 & 1 \end{bmatrix} + \mathrm{diag}\left(\mathbf{M} \begin{bmatrix} x_3 \\ x_4 \end{bmatrix} \right) \begin{bmatrix} 0 & 1 \\ j & 0 \end{bmatrix},$$

with

$$\mathbf{M} = \frac{1}{\sqrt{5}} \begin{bmatrix} \alpha & \alpha\theta \\ \bar{\alpha} & \bar{\alpha}\bar{\theta} \end{bmatrix}.$$

Since θ is the golden ratio, this code is termed as the optimal *Golden code* [39]:

$$\tilde{\mathbf{S}}(\mathbf{x}) = \frac{1}{\sqrt{5}} \begin{bmatrix} \alpha(x_1 + x_2\theta) & \alpha(x_3 + x_4\theta) \\ j\bar{\alpha}(x_3 + x_4\bar{\theta}) & \bar{\alpha}(x_1 + x_2\bar{\theta}) \end{bmatrix}, \tag{7}$$

As shown in (7), the data $\mathbf{x} = [x_1, \ldots, x_4]^\top$ are split into two groups $[x_1, x_2]^\top$ and $[x_3, x_4]^\top$, that is, the former is encoded along the diagonal line $(\tilde{s}_{11}, \tilde{s}_{22})$ and the latter is encoded along the anti-diagonal line $(\tilde{s}_{12}, \tilde{s}_{21})$.

C. RA-PTC Construction With Givens Rotation

Even though the algebraic code constructed by using the cyclic division algebra achieves optimal performance in physical-layer MIMO systems, this code should be reinvented to combat random erasures appeared in the end-to-end virtual MIMO transmission due to energy shortage of energy-harvesting devices. Specifically, considering the effect of erasures, the equivalent coded data in the bth time interval is $\mathbf{S}(\mathbf{x}) \circ \mathbf{V}_b$. It can be seen that certain entries of the coded data may be nulled, and thus the transmission reliability may be degraded.

As can be seen from (6), an entry of the algebraic code $\tilde{\mathbf{S}}(\mathbf{x})$ relates to only a fraction of $\mathbf{x}$. Taking the Golden code in (7) as an example, the diagonal coded entries $(\tilde{s}_{11}, \tilde{s}_{22})$ and the off-diagonal coded entries $(\tilde{s}_{12}, \tilde{s}_{21})$ respectively encode (x_1, x_2) and (x_3, x_4). If the erasures happen to be on the diagonal positions, (x_1, x_2) are completely erased. This implies that some entries of $\mathbf{x}$ may be completely lost only due to the presence of few erasures. To overcome this hurdle, we disperse every entry of $\mathbf{x}$ throughout the coded data by applying a rotation. The resulting RA-PTC is thus based on the Golden code and a rotation matrix, and takes the form of

$$\mathbf{S}(\mathbf{x}) = \tfrac{1}{\sqrt{5}} \begin{bmatrix} \cos\phi & -\sin\phi \\ \sin\phi & \cos\phi \end{bmatrix} \cdot \begin{bmatrix} \alpha(x_1 + x_2\theta) & \alpha(x_3 + x_4)\theta \\ j\bar{\alpha}(x_3 + x_4\bar{\theta}) & \bar{\alpha}(x_1 + x_2\bar{\theta}) \end{bmatrix}. \tag{8}$$

In this case, all entries $(x_1, \ldots, x_4)$ of the data $\mathbf{x}$ is successfully received even when only a coded symbol arrives at the destination node.

The Givens rotation can be used for a more general case with $R > 2$. Specifically, the Givens rotation can be realized by multiplying by a unitary matrix $\mathbf{G}(m, n, \phi_{m,n})$, whose (p, q)th entry $G_{p,q}(m, n, \phi_{m,n})$ is

$$G_{i,j}(m, n, \phi_{m,n}) = \begin{cases} 1, & \text{if } p = q,\ p \neq m, n, \\ \cos\phi_{m,n}, & \text{if } p = q = m \text{ or } p = q = n, \\ \sin\phi_{m,n}, & \text{if } p = m,\ q = n, \\ -\sin\phi_{m,n}, & \text{if } p = n,\ q = m, \\ 0, & \text{otherwise.} \end{cases}$$

The $R \times R$ RA-PTC is therefore constructed by sequentially multiplying by $\binom{R}{2}$ Givens rotation matrices as

$$\mathbf{S}(\mathbf{x}) = \prod_{m=1}^{R} \prod_{n=m+1}^{R} \mathbf{G}(m, n, \phi_{m,n}) \tilde{\mathbf{S}}(\mathbf{x}). \tag{9}$$

Since Givens rotation matrices are unitary, we have $\mathrm{rank}\big(\mathbf{S}(\mathbf{x})\big) = \mathrm{rank}\big(\tilde{\mathbf{S}}(\mathbf{x})\big)$ and $\det\big(\mathbf{S}(\mathbf{x})\big) = \det\big(\tilde{\mathbf{S}}(\mathbf{x})\big)$, where $\mathrm{rank}(\cdot)$ and $\det(\cdot)$ respectively indicate the rank and determinant of a matrix. Therefore, RA-PTC preserves the superior coding gain and diversity gain that the algebraic code achieves [25]. In addition, the Givens rotation can be efficiently realized by the CORDIC algorithm [40], leading to low encoding complexity.

IV. CYCLIC POWER CONTROL

Suppose that the energy harvesting activity of the nodes in the rth path enables them to transmit w symbols of $\mathbf{s}_r$.

The diversity is easily lost when the source node applies the traditional power control of (2). For example, assume that the energy harvesting result permits the transmission of $R-1$ coded symbols for all relay paths, i.e., $s_{r,1},\ldots,s_{r,R-1}$, for $r=1,\ldots,R$. Although only one symbol is lost in each relay path, the last row vector of the erasure matrix is nulled (i.e., $v_{b,R,w}=0$ for $w=1,\ldots,R$) and thus $\mathbf{\Delta}\circ\mathbf{V}_b$ becomes rank deficient, leading to diversity loss. We will formally discuss this issue in Sec. V-A.

To alleviate the diversity loss, we propose a cyclic power control which adjusts the erasure positions. The cyclic power control works as follows: When the nodes in the rth path harvest sufficient energy to transmit w symbols, the energy is allocated to relay the following symbols:

$$s_{r,r+b-1},\ldots,s_{r,\mathrm{mod}(r+w+b-1,R)}, \tag{10}$$

which implies that the data in the diagonal line of $\mathbf{S}$ has the highest priority for transmission. Consider the case of $R=4$ as an example and assume that the minimal energy harvested by the relay nodes in the third path is only sufficient for the transmission of half of the coded data in this time interval. When the cyclic power control is adopted, the destination node receives nothing but noise from the third relay path at the first and second time instants since the relay node with minimal harvested energy discards the first two symbols of the coded data. Then $s_{3,3}$ and $s_{3,4}$ are received at the third and fourth time instants, respectively. Likewise, if the fourth path can only relay half of the coded data, $s_{4,1}$ and $s_{4,4}$ are transmitted at the first and the fourth time instants, respectively.

The cyclic power control significantly mitigates the diversity loss caused by the shortage of harvested energy. To explain the diversity loss of the traditional power control, we sort the columns $\mathbf{v}_{r,b}$ in $\mathbf{V}_b$ in descending order of $\|\mathbf{v}_{r,b}\|_0$, where $\|\cdot\|_0$ denotes the l^0-norm (or Hamming weight) of a vector. Then, we have the necessary condition of full diversity: the entries of the lower triangular part of such sorted erasure matrix are all nonzeros. This means that at least one relay path should transmit the entire coded data, while the other paths need to respectively transmit at least $R-1, R-2,\ldots,1$ symbols of the coded data. With the aid of this cyclic power control, even if only a single symbol of the coded data is transmitted for each relay path, full diversity is preserved, since the diagonal terms of $\mathbf{V}_b$ are all nonzeros.

It should be emphasized that, for the cyclic power control, each relay node allocates its transmission power to various symbols simply on the basis of the amount of its harvested energy, without the necessity of exchanging the global energy-harvesting information and considering the transmission policy of other nodes. Consequently, the power control proposed in this work can be efficiently implemented in a distributive manner. Additionally, the cyclic power control can be combined with different types of PTCs, not only the RA-PTC.

V. Analysis of the Proposed RA-PTC Virtual MIMO

To provide further insight into the end-to-end RA-PTC-based virtual MIMO transmission for networks formed by energy-harvesting devices, its performance is analyzed in this section. Through the derivation of PEP, we first calculate the diversity. The diversity gain is studied for three reasons: First, the error rate performance exponentially decreases with respect to the diversity as the SNR increases. Thus, the diversity is necessary to fully characterize the performance. Second, through the analysis of the diversity, we can quantify the performance loss caused by insufficient harvested energy at different SNR regimes. Last, since the RA-PTC aims at simultaneously exploiting the path diversity and time diversity, the study of diversity gains can directly examine the effectiveness of the proposed techniques. Then, the amount of fading is analyzed to show that RA-PTC indeeds mitigates the severity of cascaded fading and erasure.

A. Diversity

The diversity gain comes into picture when transmission outage occurs so that the received equations do not possess sufficient "rank" to recover the data. Specifically, the source node encodes and transmits RB data symbols by using B time intervals and R relay paths. In each time interval, the destination node receives the symbols with the dimensions R^2 from R time instants and R relay paths. As will be expounded later, by using the proposed RA-PTC and the cyclic power control, up to R^2-R erasures (i.e., transmission outages) can be tolerated without loss of the diversity gain RB. To analyze the diversity, we define PEP

$$f(\mathbf{x}\to\hat{\mathbf{x}})=P\big(\Lambda(\mathbf{x},\hat{\mathbf{x}})<0\big) \tag{11}$$

as the probability that when the data $\mathbf{x}$ is transmitted, $\hat{\mathbf{x}}$ at the receiver has a likelihood larger than that of $\mathbf{x}$, i.e., the probability that $\mathbf{x}$ is erroneously detected as $\hat{\mathbf{x}}$ "only if" $\mathbf{x}$ and $\hat{\mathbf{x}}$ are the only two alternatives. In (11), $\Lambda(\mathbf{x},\hat{\mathbf{x}})$ denotes the log-likelihood ratio (LLR) of the joint probability density functions (PDFs) $P(\mathbf{y}_1,\ldots,\mathbf{y}_B|\mathbf{x})$ and $P(\mathbf{y}_1,\ldots,\mathbf{y}_B|\hat{\mathbf{x}})$. The following result shows the Chernoff bound of the PEP.

Lemma 1: Letting $\mathbf{\Delta}=\mathbf{S}(\mathbf{x})-\mathbf{S}(\hat{\mathbf{x}})$ be the differences between the transmitted coded data and the coded data associated with the erroneously-detected $\hat{\mathbf{x}}$, the Chernoff upper bound of the PEP (11) is given by

$$f_{\mathrm{CB}}(\mathbf{x}\to\hat{\mathbf{x}})=\prod_{b=1}^{B}\prod_{r=1}^{\mathrm{rank}(\mathbf{\Delta}\circ\mathbf{V}_b)}\exp\left(-\frac{\delta_{b,r}^2}{4\sigma_x^2}\gamma_{b,r}\right), \tag{12}$$

where σ_x^2 is the variance of an entry in $\mathbf{x}$ and $\delta_{b,r}$ is the singular value of $\mathrm{rank}(\mathbf{\Delta}\circ\mathbf{V}_b)$. The scalars

$$\gamma_{b,r}=\frac{|q_{b,r}|^2\sigma_x^2}{N_{b,0}} \tag{13}$$

represent the effective signal-to-noise ratios (SNRs), where $q_{b,r}$ is the rth entry of the equivalent fading vector $\mathbf{q}_b=\mathbf{U}_b\mathbf{h}_b$ with $\mathbf{U}_b$ being a unitary matrix.

Proof: The proof is given in Appendix A. ■

Using Lemma 1, the following theorem can be proved.

Theorem 1: The end-to-end RA-PTC transmission with repetition transmission for networks formed by energy-harvesting devices under the slow-fading channel achieves

diversity d, where

$$d = \sum_{b=1}^{B} \text{rank}(\mathbf{\Delta} \circ \mathbf{V}_b) \leq RB. \quad (14)$$

Proof: The PEP in (12) can be reformulated as

$$f_{\text{CB}}(\mathbf{x} \to \hat{\mathbf{x}}) = \left(\exp\left(-\frac{\bar{\delta}}{4\sigma_x^2} \gamma_{b,r} \right) \right)^{\sum_{b=1}^{B} \text{rank}(\mathbf{\Delta} \circ \mathbf{V}_b)}, \quad (15)$$

where $\bar{\delta} = \frac{1}{\sum_{b=1}^{B} \text{rank}(\mathbf{\Delta} \circ \mathbf{V}_b)} \sum_{b=1}^{B} \sum_{r=1}^{\text{rank}(\mathbf{\Delta} \circ \mathbf{V}_b)} \delta_{b,r}^2$ is the mean of all the nonzero singular values of $\text{rank}(\mathbf{\Delta} \circ \mathbf{V}_b)$ for $b = 1, \ldots B$. Then, we have the diversity in (14), which represents the replica of the transmitted signals, i.e., the exponent of the error rate function for a specific SNR value [36]. ■

Remark 1: Theorem 1 implies that, although the RA-PTC provides full rank of $\mathbf{\Delta}$ ($\text{rank}(\mathbf{\Delta}) = R$) for any pair $(\mathbf{S}, \hat{\mathbf{S}})$, the diversity d may be less than the maximum value RB due to erasures caused by energy shortage. For example, when $\mathbf{s}_r(\mathbf{x})$ transported through the rth relay path is completely erased in the bth time interval, as reflected by the rth column of $\mathbf{V}_b$ being nulled, we have $\text{rank}(\mathbf{\Delta} \circ \mathbf{V}_b) < R$. For a single transmission (i.e., $B = 1$), the maximal achievable diversity is only R. Such diversity may be insufficient to provide reliable end-to-end transmission when the number of adopted relay paths is small. This demonstrates the need of some kind of repetition transmission.

B. Average Diversity With Energy Arrival Statistic

The diversity shown in Theorem 1 depends on the erasure matrix $\mathbf{V}_b$. If the energy arrival statistic is taken into account, we may average this diversity over $\mathbf{V}_b$ to obtain the *expected diversity*.

We first derive the erasure statistics according to the channel capacity and the energy arrival statistics in the following Lemma.

Lemma 2: The probability of the event that w portions of the coded data can be transmitted through the rth path in the bth time interval is represented by

$$P(\|\mathbf{v}_{b,r}\|_0 = w) = \prod_{k=1}^{K_r - 1} \left(1 - F_{E_{b,r,k}}\left(N_{0,b}(2^{w\ M} - 1) \right) \right) - \prod_{k=1}^{K_r - 1} \left(1 - F_{E_{b,r,k}}\left(N_{0,b}(2^{(w+1)\ M} - 1) \right) \right), \quad (16)$$

where M is the modulation order and

$$F_{E_{b,r,k}}(x) = \sum_{n=1}^{\infty} \sum_{j=0}^{\lfloor x \rfloor} (-1)^j \binom{n}{j} (x - j)^n \frac{1}{n!} \frac{(\lambda_{b,r,k} L_{\text{E}})^n e^{-\lambda_{b,r,k} L_{\text{E}}}}{n!} \quad (17)$$

is the cumulative distribution function (CDF) of $E_{b,r,k}$ with $\lfloor \cdot \rfloor$ being the floor function.

Proof: The proof is given in Appendix B. ■

Remark 2: The erasure statistics are critical to quantify the channel quality and to realize an efficient optimal decoder at the destination node. Specifically, since the erasures occur randomly, the destination node has to jointly identify the erasures and decode the data. When the destination node applies the optimal maximum *a posteriori* (MAP) decoding algorithm, the erasure statistics derived in (16) and (17) can be used as the *a priori* information of the erasures to improve the error rate performance. By properly integrating this *a priori* information into a sphere decoding algorithm [41], an efficient optimal joint decoding (JSD) procedure can be realized [17], [18].

With the aid of Lemma 2, the following result shows the expected diversity gain of the end-to-end RA-PTC transmission with cyclic power control.

Theorem 2: Assume that all relay nodes have the same energy-harvesting statistics in all time intervals and thus $(K_r, N_{0,b}, E_{b,r,k}) = (K, N_0, E)$. For the end-to-end RA-PTC transmission with cyclic power control, we can calculate its expected diversity $\bar{d}$ by taking the expectation of d in (14) with respect to the erasure matrix $\mathbf{V}_b$ for $b = 1, \ldots, B$. Then,

$$\bar{d} = E[d] \approx RB\left(1 - (K - 1)F_E(N_0(2^M - 1))\right), \quad (18)$$

where $E[\cdot]$ denotes expectation.

Proof: The proof is given in Appendix C. ■

Remark 3: Theorem 2 implies that when more relay nodes are used in a relay path, less diversity is expected. The reason is that, whenever the harvested energy of a certain relay node is insufficient for transmission, the associated relay path can be regarded as disconnected, leading to the diversity loss.

C. Amount of Fading

In this subsection, we show that RA-PTC reshapes the statistics of the slow-fading gains in the sense of reducing the severity of fading. Such phenomenon has been investigated for fast-fading channels [19] but not for slow-fading channels. Intuitively, from (13), the entries of equivalent fading vector $\mathbf{q}_b = \mathbf{U}_b \mathbf{h}_b$ are weighted sums of R independent complex variables. Due to the central limit theorem, the real and imaginary parts $\text{Re}\{q_{b,r}\}$ and $\text{Im}\{q_{b,r}\}$ for all r converge to Gaussian random variables as $R \to \infty$, and thus the equivalent fading approaches Rayleigh fading as R grows large, as depicted in Fig. 4.

We now examine the reshaping effect that RA-PTC has on fading by deriving $\alpha_{b,r}$, the amount of fading of the bth time interval and the rth relay path:

$$\alpha_{b,r} \triangleq \frac{E\left[\gamma_{b,r}^2\right] - E\left[\gamma_{b,r}\right]^2}{E\left[\gamma_{b,r}\right]^2}. \quad (19)$$

The amount of fading is widely accepted as a measure of the severity of the fading channel, and hence is a convenient and powerful performance index [27]. Although a formal proof is missing, it is commonly accepted that the higher the amount of fading, the worse the error rate performance is. For example, the AWGN channel, the Rayleigh fading channel, and the K-product Rayleigh fading channel respectively yield $\alpha = 0$, $\alpha = 1$, and $\alpha = 2^K - 1$ [26]. The following result provides the closed-form expression of the amount of fading:

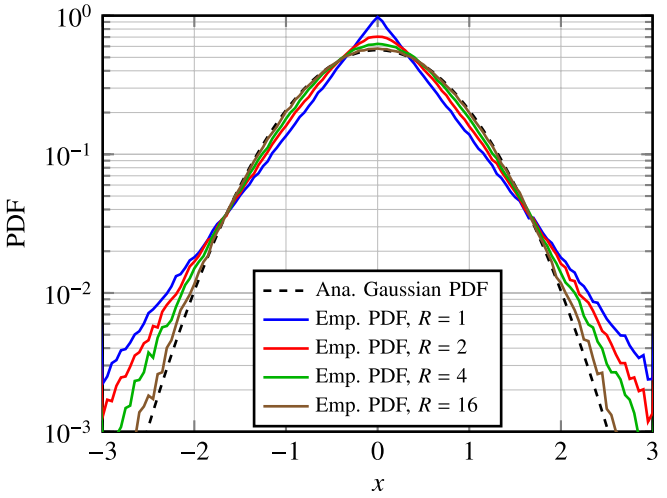

Fig. 4. Comparisons between PDF of a Gaussian random variable $N(0, 1/2)$, and empirical PDFs of $\mathrm{Re}\{q_{b,r}\}$ and $\mathrm{Im}\{q_{b,r}\}$ with $K_r = 2$ for all r and normalized channel variance.

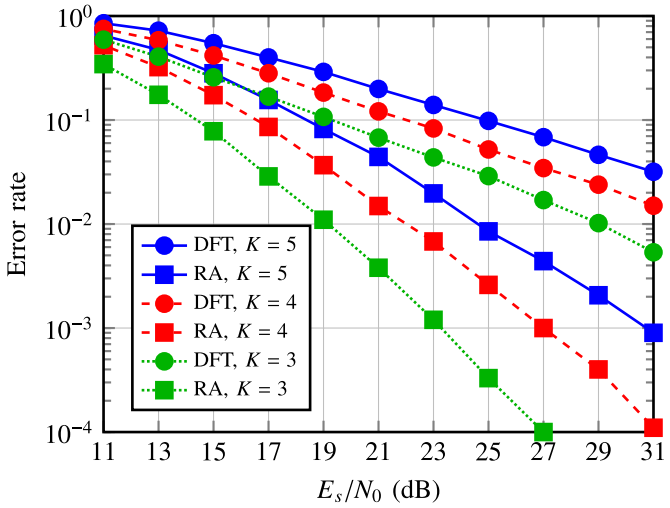

Fig. 5. Error rates of end-to-end virtual MIMO transmission based on RA-PTC and DFT-based PTC for different number of relay nodes. Cyclic power control is adopted and $(R, B) = (2, 2)$.

Lemma 3: The amount of fading reshaped by the RA-PTC is expressed as

$$\alpha_{r,b} = 1 + \sum_{r'=1}^{R} |u_{b,r',r}|^4 (2^{K_{r'}} - 2), \tag{20}$$

where $u_{b,r',r}$ is the (r', r)th entry of the unitary matrix $\mathbf{U}_b$.

Proof: The proof is given in Appendix D. ∎

Under the condition that all relay paths have the same number of links (i.e., $K_r = K$) such that the subscript r can be omitted, the following result gives a lower bound of the reshaped amount of fading.

Theorem 3: The amount of fading reshaped by the RA-PTC in (20) can be lower bounded by

$$\alpha_b \geq 1 + \frac{2^K - 2}{R}. \tag{21}$$

Proof: This is a direct consequence of the Cauchy-Schwarz inequality

$$\left(\sum_{r'=1}^{R} 1^2\right)\left(\sum_{r'=1}^{R} (|u_{b,r',r}|^2)^2\right) \geq \left(\sum_{r'=1}^{R} 1 \cdot |u_{b,r',r}|^2\right)^2 = 1, \tag{22}$$

where the last equality is due to the unitary property of $\mathbf{U}_b$. ∎

As shown in Theorem 3, although α_b increases exponentially with the number of hops K, this value is reduced when RA-PTC is adopted, thus showing the effectiveness of RA-PTC. Besides, the more relay paths, the lower the amount of fading is.

VI. Simulation Results

In this section, the performance of the proposed end-to-end virtual MIMO RA-PTC transmission for multipath, multihop networks with energy-harvesting devices is evaluated, and the analyses presented in this paper are validated by Monte Carlo simulations. The spectral efficiency of all the instances in the simulations is the same, i.e., one symbol per time instant, except some instances in Fig 6., where the number of repetitions is reduced. For those cases, the spectral efficiency increases to $\left(1 + \frac{1}{B-1}\right)$ symbols per time instant at the cost of error rate performance deterioration, as will be expounded later. For simplicity, we assume the same noise power spectral density $N_{0,b}$ for all time intervals, the same number of links K_r for all relay paths, and the same energy arrival statistics for all relay nodes. In this way, the associated subscripts can be omitted. The energy arrival follows the compound Poisson distribution, where the value of the harvested energy is a random sample from one of the corresponding i.i.d. uniformly distributed random variables with normalized support $[0, 1]$ as in [1].

Fig. 5 compares the performance of the end-to-end virtual MIMO transmission with various PTC techniques in terms of error rate for $(R, B) = (2, 2)$, where an error occurs if $\mathbf{x}$ is erroneously detected. The previously proposed discrete Fourier transform (DFT)-based PTCs [16], [17] fail to provide satisfactory error rates since they are designed for cognitive radio networks over fast-fading channels. Compared with the DFT-based PTC and subject to 1% error rate, RA-PTC achieves around 10 dB SNR performance gain for all cases.

Fig. 6 depicts the error rate of RA-PTC with various time intervals B and relay paths R. The diversity and the resulting error rate performance are enhanced when more relay paths and time intervals are introduced. We show the importance of repetition transmission by reducing the number of repetition transmissions from $B = R$ to $B = R - 1$. When the number of relay paths increases, the system is more robust to the time diversity loss caused by less repetition since the path diversity is already large enough. Comparing the cases of $(R, B) = (2, 2)$ and $(R, B) = (3, 2)$, the latter adopts one more relay path and thus provides higher throughput. However, the resulting error rate is worse than the former at most SNR regimes, demonstrating that the number of repetition transmissions can be considered as a parameter for tuning the trade-off between the error rate performance and throughput.

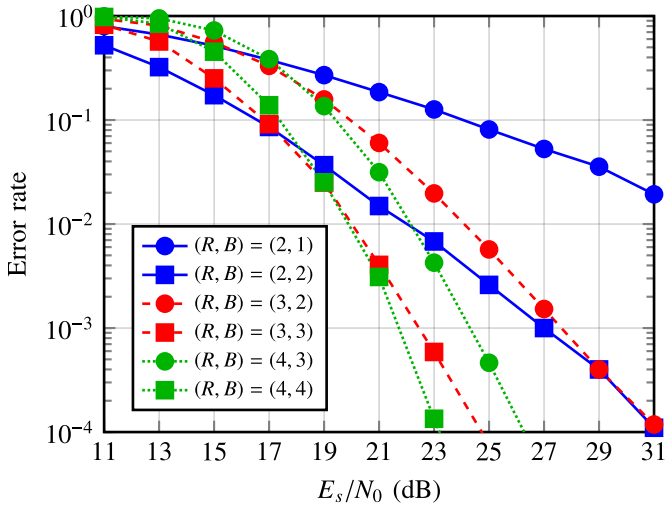

Fig. 6. Error rates of end-to-end RA-PTC transmission for various time intervals and number of relay paths. Cyclic power control is adopted and $K = 4$.

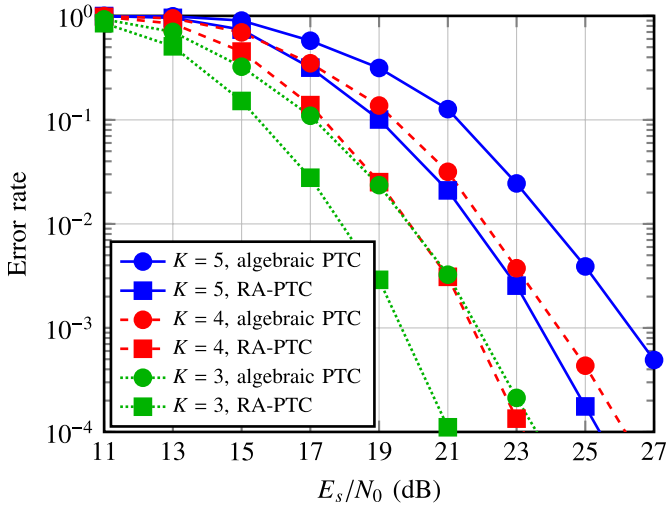

Fig. 7. Error rates of end-to-end PTC transmission with Givens rotation (i.e., RA-PTC) and without Givens rotation (i.e., algebraic PTC). Cyclic power control is adopted and $(R, B) = (4, 4)$.

In Fig. 7, we evaluate the improvement obtained by using Givens rotations. The rotated phases in (8) are heuristically optimized. Compared to the case without using rotations (i.e., algebraic PTC), the error rate performance of RA-PTC is enhanced, especially for the cases with larger K, where the erasure probability is higher as derived in Lemma 2. This phenomenon validates our discussion in Section III: Givens rotation disperses data throughout paths and relays of the network so that data becomes more robust to erasures.

Fig. 8 illustrates the performance of cyclic power control by using the diversity as the metric. The analytical expected diversity derived in Theorem 2 tightly matches the numerical result, verifying the accuracy of our closed-form expressions. Compared with the cases using the traditional power control, the cyclic power control greatly increases the diversity. Such improvement is more significant for large R and B, since the maximum diversity RB increases. When K increases, the case with cyclic power control exhibits a linear decrease of expected diversity as derived in (18), while the expected

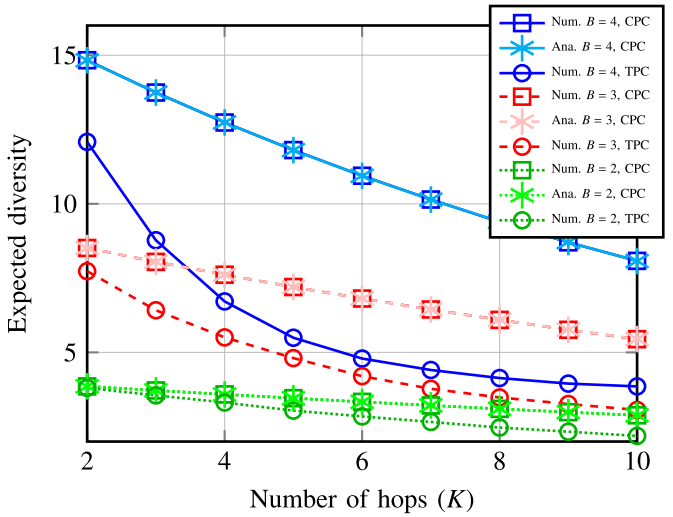

Fig. 8. Numerical and analytical diversity comparisons of end-to-end RA-PTC transmission with traditional power control (denoted as "TPC" on the figure) and cyclic power control (denoted as "CPC" on the figure) at $E_b/N_0 = 15$ dB.

diversity slumps for the case with traditional power control. Thus, the diversity gap between these two power control schemes increases as the number of relays increases. Together with other numerical results, we see that both the RA-PTC and the cyclic power control can perform well when either the number of hops or the number of relay paths increases, implying that the proposed RA-PTC virtual MIMO framework is a viable solution for large-scale networks formed by energy-harvesting devices.

VII. Conclusion

In this paper, we have considered a virtual MIMO-based open-loop end-to-end transmission framework for multipath, multihop networks formed by energy-harvesting devices, and we have introduced the RA-PTC scheme for transmissions over the slow-fading channel. By repeatedly transmitting data encoded by using Givens rotation and cyclic division algebra, the time diversity is achieved without causing any rate loss. The diversity and the amount of fading of RA-PTC have been analyzed. Furthermore, by modeling the transmission outage caused by energy-harvesting shortages as an erasure, the erasure statistics were derived and used to compute the expected diversity. These analyses shed light on the relationship among the performance, design parameters, and the energy-harvesting features. Cyclic power control has also been proposed to adjust erasure characteristics for better transmission reliability. Validated by numerical simulations, the proposed framework and schemes realize an efficient end-to-end transmission in multipath, multihop networks formed by energy-harvesting devices without needing costly end-to-end feedback and control.

Appendix

A. Derivation of Diversity

Due to the independency of the transmission in each time interval, we have

$$P(\mathbf{y}_1, \ldots, \mathbf{y}_B \mid \mathbf{x}) = \prod_{b=1}^{B} P(\mathbf{y}_b \mid \mathbf{x}) = \prod_{b=1}^{B} P(\mathbf{y}_b \mid \mathbf{S}(\mathbf{x})). \quad (23)$$

The LLR $\Lambda(\mathbf{x}, \hat{\mathbf{x}})$ is thus written as

$$\Lambda(\mathbf{x}, \hat{\mathbf{x}}) = \sum_{b=1}^{B} \Big(\log P(\mathbf{y}_b \mid \mathbf{S}(\mathbf{x})) - \log P(\mathbf{y}_b \mid \mathbf{S}(\hat{\mathbf{x}})) \Big). \quad (24)$$

Since $\mathbf{n}_b$ is AWGN with time-varying $N_{0,b}$, the PDF $P(\mathbf{y}_b|\mathbf{S}(\mathbf{x}))$ is given by

$$P(\mathbf{y}_b \mid \mathbf{S}(\mathbf{x})) = \frac{1}{\pi N_{0,b}} e^{-\frac{1}{N_{0,b}} \|\mathbf{y}_b - \mathbf{S}(\mathbf{x}) \circ \mathbf{V}_b \mathbf{h}_b\|^2}. \quad (25)$$

Inserting (25) into (24), we obtain

$$\begin{aligned} &\Lambda(\mathbf{x}, \hat{\mathbf{x}}) \\ &= \sum_{b=1}^{B} \frac{1}{N_{0,b}} \|\mathbf{y}_b - \mathbf{S}(\hat{\mathbf{x}}) \circ \mathbf{V}_b \mathbf{h}_b\|^2 - \frac{1}{N_{0,b}} \|\mathbf{y}_b - \mathbf{S}(\mathbf{x}) \circ \mathbf{V}_b \mathbf{h}_b\|^2 \\ &= \sum_{b=1}^{B} \frac{1}{N_{0,b}} \Big(\|\mathbf{\Delta} \circ \mathbf{V}_b \mathbf{h}_b\|^2 + 2 \operatorname{Re} \Big\{ \big(\mathbf{\Delta} \circ \mathbf{V}_b \mathbf{h}_b \big)^H \mathbf{n} \Big\} \Big), \end{aligned} \quad (26)$$

where $\mathbf{\Delta} = \mathbf{S}(\mathbf{x}) - \mathbf{S}(\hat{\mathbf{x}})$, and $\operatorname{Re}\{\cdot\}$ and $(\cdot)^H$ respectively denote the real part and the Hermitian conjugation. It can be seen from (26) that, conditioned on $\mathbf{h}_b$ and $\mathbf{V}_b$ for $b = 1, \ldots, B$, Λ is a Gaussian random variable with mean $\mu_\Lambda = \sum_{b=1}^{B} \frac{1}{N_{0,b}} \|\mathbf{\Delta} \circ \mathbf{V}_b \mathbf{h}_b\|^2$ and variance $\sigma_\Lambda^2 = 2\mu_\Lambda$.

The PEP derivation proceeds approximation by the Chernoff bound [42]

$$f(\mathbf{x} \to \hat{\mathbf{x}}) \approx f_{\mathrm{CB}}(\mathbf{x} \to \hat{\mathbf{x}}) = \min_t M_\Lambda(t), \quad (27)$$

where $M_\Lambda(t) = \exp\big((t + t^2)\mu_\Lambda\big)$ is the moment-generating function (MGF) of Λ. It can be verified that the minimum of $M_\Lambda(t)$ occurs at $t = -1/2$. Consequently,

$$f_{\mathrm{CB}}(\mathbf{x} \to \hat{\mathbf{x}}) = M_\Lambda\left(-\frac{1}{2}\right) = \exp\left(-\frac{\mu_\Lambda}{4}\right). \quad (28)$$

To expand (28), we reformulate μ_Λ as follows:

$$\begin{aligned} \sum_{b=1}^{B} \frac{1}{N_{0,b}} \|\mathbf{\Delta} \circ \mathbf{V}_b \mathbf{h}_b\|^2 &= \sum_{b=1}^{B} \frac{1}{N_{0,b}} \mathbf{h}_b^H (\mathbf{\Delta} \circ \mathbf{V}_b)^H (\mathbf{\Delta} \circ \mathbf{V}_b) \mathbf{h}_b \\ &\overset{(a)}{=} \sum_{b=1}^{B} \frac{1}{N_{0,b}} \mathbf{h}_b^H \mathbf{U}_b \mathbf{D}_b \mathbf{U}_b^H \mathbf{h}_b \\ &\overset{(b)}{=} \sum_{b=1}^{B} \frac{1}{N_{0,b}} \mathbf{q}_b^H \mathbf{D}_b \mathbf{q}_b \\ &\overset{(c)}{=} \sum_{b=1}^{B} \frac{1}{N_{0,b}} \sum_{r=1}^{\operatorname{rank}(\mathbf{\Delta} \circ \mathbf{V}_b)} \delta_{b,r} |q_{b,r}|^2. \end{aligned} \quad (29)$$

In (29), (a) follows from the eigendecomposition of the Hermitian matrix $\mathbf{V}_b^H \circ \mathbf{\Delta}^H \mathbf{\Delta} \circ \mathbf{V}_b$ [36], where $\mathbf{U}_b$ is a unitary matrix and $\mathbf{D}_b$ is the diagonal matrix with eigenvalues $\delta_{b,r}$ as the diagonal terms; (b) holds because of the definition of $\mathbf{q}_b = [q_{b,1}, \ldots, q_{b,R}]^\top = \mathbf{U}_b \mathbf{h}_b$; (c) follows from the fact that rank($\mathbf{A}$) is the number of nonzero eigenvalues of matrix $\mathbf{A}$. By using (29), we have (12).

B. Derivation of Erasure Statistics

Define $E_{\mathrm{T},b,w}$ as the energy threshold that a relay node needs to exceed in order to relay w symbols in the bth time interval [43]. Since this energy threshold is assumed to at least provide the channel capacity larger than the transmission rate, we have the rate condition $\log_2\left(1 + \frac{E_{\mathrm{T},b,w}}{N_{0,b}}\right) \geq wM$. Consequently, the minimum energy $E_{\mathrm{T},b,w}$ necessary for transmitting w symbols of the coded data is derived as $E_{\mathrm{T},b,w} = N_{0,b}(2^{wM} - 1)$.

Given that the energy arrival is a compound Poisson process, for the energy that the kth relay node in the rth path and the bth time interval harvests ($E_{b,r,k}$), its CDF takes the form of

$$F_{E_{b,r,k}}(x) = \sum_{n=1}^{\infty} P\left(\sum_{i=1}^{n} E_{b,r,k,i} \leq x \right) f(n; \lambda_{r,k} L_{\mathrm{E}}), \quad (30)$$

where $E_{b,r,k,i}$ denotes the value of the ith energy arrival at the kth node in the rth relay path and the bth time interval, and $n \in \mathbb{N}$ represents the number of energy arrivals, which is a Poisson random variable with its PDF $f(n; \lambda_{b,r,k} L_{\mathrm{E}})$ given by

$$f(n; \lambda_{b,r,k} L_{\mathrm{E}}) = \frac{(\lambda_{b,r,k} L_{\mathrm{E}})^n e^{-\lambda_{b,r,k} L_{\mathrm{E}}}}{n!}. \quad (31)$$

The probability $P(\sum_{i=1}^{n} E_{b,r,k,i} \leq x)$ in (30) is computed if the statistics of the energy arrival are specified. For example, if $E_{b,r,k,i}$ is uniformly distributed in [0, 1], the summation $\sum_{i=1}^{n} E_{b,r,k,i}$ has the Irwin-Hall distribution [1], whose CDF can be used to obtain

$$P\left(\sum_{i=1}^{n} E_{b,r,k,i} \leq x \right) = \sum_{j=0}^{\lfloor x \rfloor} (-1)^j \binom{n}{j} (x - j)^n \frac{1}{n!}; \quad (32)$$

$\lfloor \cdot \rfloor$ is the floor operator. Inserting (32) and (31) into (30), the CDF of the harvested energy $F_{E_{b,r,k}}(x)$ is computed as in (17). Now, letting $P(\|\mathbf{v}_r\|_0 = w)$ be the probability of the event that w portions of the coded data can be transmitted through the rth path, we have

$$\begin{aligned} P(\|\mathbf{v}_r\|_0 = w) = P\Big(& N_{0,b}(2^{w\ M} - 1) < \min\{E_{b,r,1}, \\ & \ldots, E_{b,r,K_r - 1}\} \leq N_{0,b}(2^{(w+1)\ M} - 1) \Big) \\ = & \prod_{k=1}^{K_r - 1} \Big(1 - F_{E_{b,r,k}}\big(N_{0,b}(2^{w\ M} - 1)\big) \Big) \\ & - \prod_{k=1}^{K_r - 1} \Big(1 - F_{E_{b,r,k}}\big(N_{0,b}(2^{(w+1)\ M} - 1)\big) \Big). \end{aligned} \quad (33)$$

C. Derivation of Expected Diversity

For the RA-PTC, we have full rank of $\mathbf{\Delta}$. When cyclic power control is adopted, the diversity is lost only if a certain relay path r in a certain time interval b cannot be used to propagate any message due to energy shortage. That is, among $K_r - 1$ relay nodes, at least one node has harvested

energy less than $E_{\mathrm{T},b,1} = N_{0,b}(2^M - 1)$. The probability for this event to happen can be derived as

$$P(\|\mathbf{v}_{b,r}\| = 0) = 1 - \prod_{k=1}^{K_r - 1} \left(1 - F_{E_{b,r,k}}(N_{0,b}(2^M - 1))\right) \overset{(a)}{\approx} \sum_{k=1}^{K_r - 1} F_{E_{b,r,k}}(N_{0,b}(2^M - 1)), \tag{34}$$

where (a) follows from the approximation $\prod_k (1 - a_k) \approx 1 - \sum_k a_k$ (valid for small a_k).

Assuming that all relay nodes have the same energy-harvesting statistics in all time intervals, the subscripts of b and r can be dropped, leading to

$$P(\|\mathbf{v}\| = 0) \approx (K - 1) F_E(N_0(2^M - 1)). \tag{35}$$

Then, under the assumption of independent energy-harvesting statistics, the diversity is degraded only when a null column vector $\mathbf{v}$ appears. Denoting x as the number of column vectors $\mathbf{v}$ with at least one nonzero entry, the expected diversity is computed as

$$\begin{aligned}
\bar{d} &= E[d] = \sum_{x=0}^{RB} P(x) \cdot x \\
&= \sum_{x=0}^{RB} \binom{RB}{x} P(\|\mathbf{v}\| = 0)^{RB - x} (1 - P(\|\mathbf{v}\| = 0))^x \cdot x \\
&= \big(1 - P(\|\mathbf{v}\| = 0)\big) RB \cdot \sum_{x=1}^{RB} \frac{RB - 1}{(RB - x)(x - 1)} \\
&\quad \times P(\|\mathbf{v}\| = 0)^{RB - x} \big(1 - P(\|\mathbf{v}\| = 0)\big)^{x - 1} \\
&= \big(1 - P(\|\mathbf{v}\| = 0)\big) RB \\
&\quad \cdot \sum_{x=0}^{RB-1} \binom{RB - 1}{x - 1} P(\|\mathbf{v}\| = 0)^{(RB-1) - x} \big(1 - P(\|\mathbf{v}\| = 0)\big)^x \\
&\overset{(a)}{=} RB\big(1 - P(\|\mathbf{v}\| = 0)\big) \\
&\approx RB\left(1 - (K - 1) F_E(N_0(2^M - 1))\right),
\end{aligned} \tag{36}$$

where (a) is due to the Binomial theorem.

D. Derivation of the Amount of Fading

For notational simplicity, in the following derivations, we drop the time index b. To compute the amount of fading, we first expand $|q_r|^2$ as

$$|q_r|^2 = \sum_{r'=1}^{R} |u_{r',r}|^2 |h_{r'}|^2 + 2 \sum_{r'_1=1}^{R} \sum_{r'_2=r'_1+1}^{R} |u_{r'_1,r}||u_{r'_2,r}||h_{r'_1}||h_{r'_2}| \cos(\theta_{r'_1} - \theta_{r'_2}), \tag{37}$$

where $\theta_{r'}$ denotes the phase of $h_{r'}$, and $u_{r',r}$ is the (r', r)th entry of $\mathbf{U}$. Assuming that each link experiences i.i.d. Rayleigh fading, the first few moments of the fading magnitudes $|h_r|$ can be computed as [27]

$$E[|h_r|] = \prod_{k=1}^{K_r} E\left[|g_{r,k}|\right] = \left(\frac{\pi \sigma_g^2}{4}\right)^{K_r/2}, \tag{38}$$

$$E\left[|h_r|^2\right] = \prod_{k=1}^{K_r} E\left[|g_{r,k}|^2\right] = \left(\sigma_g^2\right)^{K_r},$$

$$E\left[|h_r|^4\right] = \prod_{k=1}^{K_r} E\left[|g_{r,k}|^4\right] = 2^{K_r}\left(\sigma_g^2\right)^{2K_r}. \tag{39}$$

Since θ_r is the summation of K_r uniformly-distributed random variables with support $[-\pi, \pi]$, the random variables $\cos(\theta_{r_1} - \theta_{r_2})$ is a random variable with support $[-1, +1]$, with the first and second moments given by

$$E\left[\cos(\theta_{r_1} - \theta_{r_2})\right] = 0, \tag{40}$$

$$E\left[\cos^2(\theta_{r_1} - \theta_{r_2})\right] = \frac{1}{2}. \tag{41}$$

By using (37) and the property of the independency of $|h_r|$ and θ_r, the mean value of SNR is computed as

$$E\left[\gamma_r\right] = \frac{\sigma_x^2}{N_0} E\left[|q_r|^2\right] \overset{(a)}{=} \frac{\sigma_x^2}{N_0} \sum_{r'=1}^{R} |u_{r'r}|^2 \left(\sigma_g^2\right)^{K_r}, \tag{42}$$

where (a) follows from (38) and (40). To calculate the second moment of SNR, i.e., $E\left[\gamma_r^2\right]$, we expand $|q_r|^4$ as

$$\begin{aligned}
|q_r|^4 = &\left(\sum_{r'=1}^{R} |u_{r',r}|^2 |h_{r'}|^2\right)^2 + 2\left(\sum_{r'=1}^{R} |u_{r',r}|^2 |h_{r'}|^2\right) \\
&\times \left(2 \sum_{r'_1=1}^{R} \sum_{r'_2=r'_1+1}^{R} |u_{r'_1,r}||u_{r'_2,r}||h_{r'_1}||h_{r'_2}| \cos(\theta_{r'_1} - \theta_{r'_2})\right) \\
&+ \left(2 \sum_{r'_1=1}^{R} \sum_{r'_2=r'_1+1}^{R} |u_{r'_1,r}||u_{r'_2,r}||h_{r'_1}||h_{r'_2}| \cos(\theta_{r'_1} - \theta_{r'_2})\right)^2.
\end{aligned} \tag{43}$$

Then, the second moment of SNR is computed by

$$\begin{aligned}
E\left[\gamma_r^2\right] &\overset{(a)}{=} \left(\frac{\sigma_x^2}{N_0}\right)^2 \left(E\left[\left(\sum_{r'=1}^{R} |u_{r',r}|^2 |h_{r'}|^2\right)^2\right] \right. \\
&\quad \left. + E\left[2 \sum_{r'_1=1}^{R} \sum_{r'_2=r'_1+1}^{R} |u_{r'_1,r}|^2 |u_{r'_2,r}|^2 |h_{r'_1}|^2 |h_{r'_2}|^2\right]\right) \\
&\overset{(b)}{=} \left(\frac{\sigma_x^2}{N_b}\right)^2 \left(\sum_{r'=1}^{R} |u_{r',r}|^4 2^{K_{r'}} \left(\sigma_g^2\right)^{2K_{r'}} \right. \\
&\quad \left. + 4 \sum_{r'_1=1}^{R} \sum_{r'_2=r'_1+1}^{R} |u_{r'_1,r}|^2 |u_{r'_2,r}|^2 \left(\sigma_g^2\right)^{K_{r'_1} + K_{r'_2}}\right),
\end{aligned} \tag{44}$$

where (a) follows from (40) and (b) from (38).

The influence of K and R on the amount of fading can be shown more clearly by assuming a normalized variance of the

link gain, that is, $\sigma_g^2 = 1$. With this assumption, (42) and (44) are respectively simplified to

$$E\left[\gamma_r\right] = \frac{\sigma_x^2}{N_0}, \tag{45}$$

$$E\left[\gamma_r^2\right] \overset{(a)}{=} \left(\frac{\sigma_x^2}{N_b}\right)^2 \left(2 + \sum_{r'=1}^{R} |u_{r',r}|^4 (2^{K_{r'}} - 2)\right), \tag{46}$$

where (a) follows from

$$1 = \left(\sum_{r'=1}^{R} |u_{r',r}|^2\right)^2 = \sum_{r'=1}^{R} |u_{r',r}|^4 + 2 \sum_{r_1'=1}^{R} \sum_{r_2'=r_1'+1}^{R} |u_{r_1',r}|^2 |u_{r_2',r}|^2. \tag{47}$$

With the results derived above, we have the amount of fading expressed in (20).

REFERENCES

[1] O. Ozel, K. Tutuncuoglu, J. Yang, S. Ulukus, and A. Yener, "Transmission with energy harvesting nodes in fading wireless channels: Optimal policies," *IEEE J. Sel. Areas Commun.*, vol. 29, no. 8, pp. 1732–1743, Sep. 2011.

[2] J. Yang, O. Ozel, and S. Ulukus, "Broadcasting with an energy harvesting rechargeable transmitter," *IEEE Trans. Wireless Commun.*, vol. 11, no. 2, pp. 571–583, Feb. 2012.

[3] B. Devillers and D. Gündüz, "A general framework for the optimization of energy harvesting communication systems with battery imperfections," *J. Commun. Netw.*, vol. 14, no. 2, pp. 130–139, Apr. 2012.

[4] K. Tutuncuoglu and A. Yener, "Energy harvesting broadcast channel with inefficient energy storage," in *Proc. Asilomar Conf. Signals, Syst., Comput.*, Nov. 2012, pp. 53–57.

[5] O. Orhan, D. Gündüz, and E. Erkip, "Throughput maximization for an energy harvesting communication system with processing cost," in *Proc. IEEE Inf. Theory Workshop (ITW)*, Sep. 2012, pp. 84–88.

[6] N. Michelusi, K. Stamatiou, and M. Zorzi, "Transmission policies for energy harvesting sensors with time-correlated energy supply," *IEEE Trans. Commun.*, vol. 61, no. 7, pp. 2988–3001, Jul. 2013.

[7] B. K. Chalise, W.-K. Ma, Y. D. Zhang, H. A. Suraweera, and M. G. Amin, "Optimum performance boundaries of OSTBC based AF-MIMO relay system with energy harvesting receiver," *IEEE Trans. Signal Process.*, vol. 61, no. 17, pp. 4199–4213, Sep. 2013.

[8] S. Lee, R. Zhang, and K. Huang, "Opportunistic wireless energy harvesting in cognitive radio networks," *IEEE Trans. Wireless Commun.*, vol. 12, no. 9, pp. 4788–4799, Sep. 2013.

[9] J. Xu and R. Zhang, "Throughput optimal policies for energy harvesting wireless transmitters with non-ideal circuit power," *IEEE J. Sel. Areas Commun.*, vol. 32, no. 2, pp. 322–332, Feb. 2014.

[10] C. Huang, R. Zhang, and S. Cui, "Throughput maximization for the Gaussian relay channel with energy harvesting constraints," *IEEE J. Sel. Areas Commun.*, vol. 31, no. 8, pp. 1469–1479, Aug. 2013.

[11] K. Tutuncuoglu, B. Varan, and A. Yener, "Optimum transmission policies for energy harvesting two-way relay channels," in *Proc. IEEE Int. Conf. Commun. (ICC)*, Jun. 2013, pp. 586–590.

[12] O. Orhan and E. Erkip, "Throughput maximization for energy harvesting two-hop networks," in *Proc. IEEE Int. Symp. Inf. Theory (ISIT)*, Jul. 2013, pp. 1596–1600.

[13] R. H. Y. Louie, M. R. McKay, and I. B. Collings, "Open-loop spatial multiplexing and diversity communications in ad hoc networks," *IEEE Trans. Inf. Theory*, vol. 57, no. 1, pp. 317–344, Jan. 2011.

[14] K.-C. Chen and S.-Y. Lien, "Machine-to-machine communications: Technologies and challenges," *Ad Hoc Netw.*, vol. 18, pp. 3–23, Jul. 2014.

[15] S.-Y. Lien, S.-C. Hung, and K.-C. Chen, "Optimal radio access for fully packet-switching 5G networks," in *Proc. IEEE Int. Conf. Commun. (ICC)*, Jun. 2015, pp. 3921–3926.

[16] I.-W. Lai, C.-H. Lee, and K.-C. Chen, "A virtual MIMO path-time code for cognitive ad hoc networks," *IEEE Commun. Lett.*, vol. 17, no. 1, pp. 4–7, Jan. 2013.

[17] I.-W. Lai, C.-L. Chen, C.-H. Lee, K.-C. Chen, and E. Biglieri, "End-to-end virtual MIMO transmission in ad hoc cognitive radio networks," *IEEE Trans. Wireless Commun.*, vol. 13, no. 1, pp. 330–341, Jan. 2014.

[18] I.-W. Lai, C.-H. Lee, K. C. Chen, and E. Biglieri, "Path-permutation codes for end-to-end transmission in ad hoc cognitive radio networks," *IEEE Trans. Wireless Commun.*, vol. 14, no. 6, pp. 3309–3321, Jun. 2015.

[19] I.-W. Lai, C.-H. Lee, K. C. Chen, and E. Biglieri, "Performance of path-time codes for end-to-end transmission in ad hoc multihop networks," in *Proc. IEEE Int. Symp. Inf. Theory (ISIT)*, Jun./Jul. 2014, pp. 66–70.

[20] Y.-C. Chen, I.-W. Lai, C.-H. Lee, K.-C. Chen, and W.-T. Chen, "Transmission latency and reliability trade-off in path-time coded cognitive radio ad hoc networks," in *Proc. IEEE Global Commun. Conf. (GLOBECOM)*, Dec. 2014, pp. 1084–1089.

[21] P. Djukic and S. Valaee, "Reliable packet transmissions in multipath routed wireless networks," *IEEE Trans. Mobile Comput.*, vol. 5, no. 5, pp. 548–559, May 2006.

[22] M. K. Marina and S. R. Das, "On-demand multipath distance vector routing in ad hoc networks," in *Proc. IEEE Int. Conf. Netw. Protocol (ICNP)*, Nov. 2001, pp. 14–23.

[23] S. Fashandi, S. O. Gharan, and A. K. Khandani, "Path diversity over packet switched networks: Performance analysis and rate allocation," *IEEE/ACM Trans. Netw.*, vol. 18, no. 5, pp. 1373–1386, May 2010.

[24] B. A. Sethuraman, B. S. Rajan, and V. Shashidhar, "Full-diversity, high-rate space-time block codes from division algebras," *IEEE Trans. Inf. Theory*, vol. 49, no. 10, pp. 2596–2616, Oct. 2003.

[25] F. Oggier, J.-C. Belfiore, and E. Viterbo, "Cyclic division algebras: A tool for space–time coding," *Found. Trends Commun. Inf. Theory*, vol. 4, no. 1, pp. 1–95, 2007.

[26] G. K. Karagiannidis, N. C. Sagias, and P. T. Mathiopoulos, "N_*Nakagami: A novel stochastic model for cascaded fading channels," *IEEE Trans. Commun.*, vol. 55, no. 8, pp. 1453–1458, Aug. 2007.

[27] M. K. Simon and M.-S. Alouini, *Digital Communications Over Fading Channels*. New York, NY, USA: Wiley, 2005.

[28] B. K. Chalise, Y. D. Zhang, and M. G. Amin, "Energy harvesting in an OSTBC based amplify-and-forward MIMO relay system," in *Proc. IEEE Int. Conf. Acoust., Speech, Signal Process.*, Mar. 2012, pp. 3201–3204.

[29] Q. Zhang, Q. Li, and J. Qin, "Beamforming design for OSTBC based AF-MIMO two-way relay networks with simultaneous wireless information and power transfer," *IEEE Trans. Veh. Technol.*, to be published.

[30] W.-C. Ao and K.-C. Chen, "End-to-end HARQ in cognitive radio networks," in *Proc. IEEE Wireless Commun. Netw. Conf. (WCNC)*, Apr. 2010, pp. 1–6.

[31] P.-Y. Chen, W.-C. Ao, and K.-C. Chen, "Rate-delay enhanced multipath transmission scheme via network coding in multihop networks," *IEEE Commun. Lett.*, vol. 16, no. 3, pp. 281–283, Mar. 2012.

[32] D. Saha, S. Roy, S. Bandyopadhyay, T. Ueda, and S. Tanaka, "An adaptive framework for multipath routing via maximally zone-disjoint shortest paths in ad hoc wireless networks with directional antenna," in *Proc. IEEE Global Commun. Conf. (GLOBECOM)*, Dec. 2003, pp. 226–230.

[33] Y.-H. Wang, H.-Z. Lin, and S.-M. Chang, "Interfering-aware QoS multipath routing for ad hoc wireless network," in *Proc. IEEE Int. Conf. Adv. Inf. Netw. Appl.*, Mar. 2004, pp. 29–34.

[34] S. Ju and J. B. Evans, "Cognitive multipath multi-channel routing protocol for mobile ad-hoc networks," in *Proc. IEEE Global Commun. Conf. (GLOBECOM)*, Dec. 2003, pp. 1–6.

[35] Y. Jing and B. Hassibi, "Distributed space-time coding in wireless relay networks," *IEEE Trans. Wireless Commun.*, vol. 5, no. 12, pp. 3524–3536, Dec. 2006.

[36] V. Tarokh, N. Seshadri, and A. R. Calderbank, "Space–time codes for high data rate wireless communication: Performance criterion and code construction," *IEEE Trans. Inf. Theory*, vol. 44, no. 2, pp. 744–765, Mar. 1998.

[37] D. Gesbert, M. Shafi, D.-S. Shiu, P. J. Smith, and A. Naguib, "From theory to practice: An overview of MIMO space–time coded wireless systems," *IEEE J. Sel. Areas Commun.*, vol. 21, no. 3, pp. 281–302, Apr. 2003.

[38] H. Bölcskei and A. J. Paulraj, "Performance of space-time codes in the presence of spatial fading correlation," in *Proc. 34th Asilomar Conf. Signals, Syst., Comput.*, Oct./Nov. 2010, pp. 687–693.

[39] J.-C. Belfiore, G. Rekaya, and E. Viterbo, "The golden code: A 2×2 full-rate space-time code with nonvanishing determinants," *IEEE Trans. Inf. Theory*, vol. 51, no. 4, pp. 1432–1436, Apr. 2005.

[40] T.-D. Chiueh, P.-Y. Tsai, and I.-W. Lai, *Baseband Receiver Design for Wireless MIMO-OFDM Communications*, 2nd ed. New York, NY, USA: Wiley, 2012.

[41] C. P. Schnorr and M. Euchner, "Lattice basis reduction: Improved practical algorithms and solving subset sum problems," *Math. Program.*, vol. 66, nos. 1–3, pp. 181–191, Aug. 1994.
[42] G. Caire, G. Taricco, and E. Biglieri, "Bit-interleaved coded modulation," *IEEE Trans. Inf. Theory*, vol. 44, no. 3, pp. 927–946, May 1998.
[43] O. Ozel and S. Ulukus, "Achieving AWGN capacity under stochastic energy harvesting," *IEEE Trans. Inf. Theory*, vol. 58, no. 10, pp. 6471–6483, Oct. 2012.

I-Wei Lai (M'11) received the Ph.D. degree in electrical engineering from the Graduate Institute of Electronics Engineering (GIEE), National Taiwan University, in 2011. He was a Research Assistant with the Institute of Integrated Signal Processing Systems, RWTH Aachen University, Germany. He is currently an Assistant Professor with Chang Gung University, Taiwan. His research interests include baseband signal processing, optimization, MIMO communication, and ad hoc cognitive radio network. He was a recipient of the NTU-GIEE Best Thesis Award in 2011 for his Ph.D. thesis and is a Member of the Phi Tau Phi Scholastic Honor Society. He was recognized as an Exemplar Reviewer of the IEEE TRANSACTIONS ON COMMUNICATIONS in 2014.

Chia-Han Lee received the B.S. degree from National Taiwan University, Taipei, Taiwan, in 1999, the M.S. degree from the University of Michigan, Ann Arbor, in 2003, and the Ph.D. degree from Princeton University in 2008, all in electrical engineering. From 1999 to 2001, he served in the Republic of China Army as a Missile Operation Officer. From 2008 to 2009, he was a Post-Doctoral Research Associate with the University of Notre Dame, USA. Since 2010, he has been with Academia Sinica as an Assistant Research Fellow. His research interests include wireless communications and networks. He is an Editor of the IEEE TRANSACTIONS ON WIRELESS COMMUNICATIONS and the IEEE COMMUNICATIONS LETTERS.

Kwang-Cheng Chen (M'89–SM'94–F'07) received the B.S. from the National Taiwan University in 1983, and the M.S. and Ph.D from the University of Maryland, College Park, USA, in 1987 and 1989, all in electrical engineering. From 1987 to 1998, He worked with SSE, COMSAT, IBM Thomas J. Watson Research Center, and National Tsing Hua University, working on the mobile communications and networks. Since 1998, he has been with the National Taiwan University, Taipei, Taiwan, ROC. After serving as the Director, Graduate Institute of Communication Engineering, Communication Research Center, and the Associate Dean for Academic Affairs, he is a Distinguished Professor with the National Taiwan University and is visiting the Massachusetts Institute of Technology during 2015–2016. He has been actively involving in the organization of various IEEE conferences as General/TPC Chair/Co-Chair, and has served in editorships with a few IEEE journals. He also actively participates in and has contributed essential technology to various IEEE 802, Bluetooth, and LTE and LTE-A wireless standards. Dr. Chen is an IEEE Fellow and has received a number of awards such as the 2011 IEEE COMSOC WTC Recognition Award, 2014 IEEE Jack Neubauer Memorial Award and 2014 IEEE COMSOC AP Outstanding Paper Award. His recent research interests include wireless communications, network science, and data science.

Ezio Biglieri (M'73–SM'82–F'89–LF'10) was born in Aosta, Italy. He received the D.Eng. degree from the Politecnico di Torino, Italy, in 1967. He received his training in electrical engineering from the Politecnico di Torino. Among other honors, he received the IEEE Donald G. Fink Prize Paper Award (2000), the IEEE Third-Millennium Medal (2000), the IEEE Communications Society Edwin Howard Armstrong Achievement Award (2001), the *Journal of Communications and Networks* Best Paper Award (2004 and 2012), the IEEE Information Theory Society Aaron D. Wyner Distinguished Service Award (2012), and the EURASIP Athanasios Papoulis Award for outstanding contributions to education in communications and information theory (2013). He was elected three times to the Board of Governors of the IEEE Information Theory Society. In 1999, he was the President of the IEEE Information Theory Society. He is serving on the Scientific Board of the French company Sequans Communications, and until 2012, he was a member of the Scientific Council of the Groupe des Ecoles des Telecommunications, France. Since 2011, he has been a member of the Scientific Advisory Board of the European Coordinated Research on Long-Term Challenges in Information and Communication Sciences & Technologies ERANet. He was the Editor-in-Chief of the IEEE TRANSACTIONS ON INFORMATION THEORY, the IEEE COMMUNICATIONS LETTERS, the *European Transactions on Telecommunications*, and the *Journal of Communications and Networks*.